Sensitivity of localized surface plasmon resonances to bulk and local changes in the optical environment

W. Andrew Murray, Baptiste Auguié and William L. Barnes*

School of Physics, University of Exeter, Stocker Road, Exeter, EX4 4QL, UK, EU

Email: w.a.murray@ex.ac.uk

Abstract

Single rod-shaped and disc-shaped gold nanoparticles with sizes ranging from 60 nm up to 162 nm were analyzed using dark-field scattering spectroscopy. The sensitivity of the localized surface plasmon resonance (LSPR) of each nanoparticle to both a bulk and a local change in the refractive index of the environment was obtained by monitoring the change in the spectral position of the LSPR. It was found that the rods were more sensitive to changes in both the local environment and the bulk environment, in particular for rods with a length > 110 nm. This behaviour was confirmed by finite element modelling of the structures that clearly indicated a saturation of the relative wavelength shift for the discs as the diameter increased whereas the sensitivity of the rods continued to increase linearly with increasing length. This disparity in the behaviour of the two types of nanoparticle may in part be attributed to two principal effects associated with the presence of the substrate. Firstly, that the proportion of the surface area of the nanoparticle in contact with the substrate is larger for the disc than for the rod; secondly, that the LSPR electromagnetic field is more concentrated within the superstrate for the rod compared to the disc. Further analysis of data obtained from modelling a changing local environment indicates that, although the rods are more sensitive, both rods and discs exhibit a similar field confinement.

KEYWORDS: gold, nanoparticles, sensing, plasmonics

Introduction

Gold and silver nanoparticles have been widely studied during the past 20 years owing to their interesting optical properties [1-4]. A resonant oscillation of the conduction electrons within the nanoparticle gives rise to enhanced scattering and absorption of light, typically within the visible/near-infrared region of the electromagnetic spectrum. Referred to as the localized surface plasmon resonance (LSPR), its position in wavelength is dependent on the composition of the nanoparticle, the size and the shape of the nanoparticle [2,5-7] and nanoparticle interactions [8,9]. Furthermore it is well known that when the environment surrounding a nanoparticle is altered in some way the spectral position of the LSPR is altered. It is this last characteristic of the LSPR that has attracted the most interest and research effort since the sensitivity of the LSPR (in particular how far the peak in the LSPR spectrum moves) to a change in nanoparticle environment depends on a number of factors such as size, shape and composition[10]. Moreover, the volume around the nanoparticle within which an environmental change will induce an LSPR shift extends only a few tens of nanometers from the nanoparticle surface[11,12]. In particular this very small sensing volume can lead to the application of metallic nanoparticles as biological sensors[13-17]. A further consideration is how best to functionalize a surface for use in biosensing applications. In this respect Au nanoparticles have a number of advantages principally the gold-thiol (Au-SH) chemistry for surface functionalization. This, coupled with its low absorption relative to other metals in the visible spectral regime, and general robustness, indicates that Au is a good choice as a material for use in plasmonic biosensors.

For simple shapes such as spheres or ellipsoids the extent of the LSPR wavelength shift is typically between 100 and 200 nm per refractive index unit (RIU) when the bulk medium surrounding the nanoparticle is changed[16]. A shift per refractive index unit is defined as the shift in nm of the LSPR peak that would occur if the refractive index of the bulk medium surrounding the nanoparticle is changed by 1. Recent advances in fabrication procedures have permitted the production of more exotic

shapes such as ring structures[18], star-shaped nanoparticles[19] and core-shell structures including spherical[20] and elongated rice-shaped nanoparticles[21]. In particular the star-shaped nanoparticles have LSPRs that are remarkably sensitive, exhibiting a shift of 665 nm/RIU. Although exhibiting an even larger LSPR shift, the rice-shaped nanoparticles have a rather broad resonance – narrow spectral linewidths are desirable since for a given shift in the peak position a larger change in signal will be detected compared to a broad resonance[16]. To address the influence of LSPR linewidth on nanoparticle sensitivity a figure of merit (FOM) was introduced that is simply the relative shift of the LSPR *m* in units of eV/RIU divided by the linewidth (full width half maximum (FWHM)) in eV[22]

$$FOM = \frac{m}{FWHM}.$$

Although going some way to indicating optimum nanoparticle design this approach does not take into account how the intensity of the detected light changes when the external environment is altered. For instance, if the radiation pattern of a nanoparticle changes the amount of light detected may be altered, particularly in measurements where only scattered light is detected. In addition, when using the FOM calculation there is no consideration of how a thin layer may influence the position of the LSPR – some nanoparticles may be more sensitive to a change in the environment local to the nanoparticle than others[11,23]. The local sensitivity is determined by how confined the enhanced electromagnetic field associated with the LSPR is to the surface of the nanoparticle and varies according to the size and shape of the nanoparticle.

Some interesting questions arise when one considers which are the factors that cause the variation in the sensitivity of the LSPR position to an external change. Firstly, to what extent is the electromagnetic field confinement influenced by increasing curvature at a surface[24]? It has been observed that for nanoparticles composed of a single material it is those with the sharpest tips that exhibit the highest sensitivity (largest relative shift), such as star-shaped nanoparticles[19]. Secondly, with substrate-supported nanoparticles what proportion of the LSPR electromagnetic field is distributed within the

substrate? If this is increased for some nanoparticles compared to others then the relative sensitivity of the LSPR would be reduced[18]. It has been shown that substrate supported nanoparticles are less sensitive to a bulk change than nanoparticles in a homogeneous environment because some of the electromagnetic field associated with the LSPR is contained within the substrate[25]. Also, nanoparticles embedded in a polymer matrix are less sensitive for similar reasons[26]. Thirdly, how much influence do the intrinsic material properties of the nanoparticle (such as the relative permittivity) have in dictating the nanoparticle sensitivity? The way in which the real and imaginary parts of the relative permittivity of Au and Ag vary with wavelength/frequency will influence the overall sensitivity of the LSPR[27]. Indeed, for nanoparticles embedded within a homogeneous medium and with a size < 120 nm numerical modelling techniques supplemented by simple electrostatic analysis have been used to suggest that it is solely the spectral position of the LSPR that dictates its sensitivity to an external change[27].

There are two kinds of change in the environment of a nanoparticle that are of interest: (1) a bulk change, when the entire environment of the nanoparticle is changed and (2) a local change, for example when a thin layer of material is deposited onto the nanoparticle. The latter definition has particular significance within biosensing where typically either direct adsorption of molecules onto a nanoparticle or adsorption onto a receptor or host molecule induces the LSPR shift. In these types of experiment the location of a binding event can have a significant influence upon the size of this shift; if the target molecule binds at the center of the nanoparticle where the electromagnetic field intensity is relatively low a smaller shift will be induced than if the target molecule binds at, for instance, the tips of a triangular nanoparticle where the field is most intense[28]. For clarity, here we consider thin to be of the same order as the decay length of the electromagnetic field associated with the LSPR, typically a few tens of nanometers. Interference effects in layers with a thickness approaching that of an optical path length may also lead to LSPR shifts[12,29]. Whilst a nanoparticle that exhibits a high sensitivity to a bulk change may indicate a high sensitivity to a local change, it has been shown previously that it is possible

for nanoparticles with a moderate bulk sensitivity to exhibit a local sensitivity comparable to or exceeding that of nanoparticles with a higher bulk sensitivity[11]. Therefore to determine fully the effectiveness of a nanoparticle as a sensor it is necessary to evaluate both the bulk and local sensitivities to a change in environment. Moreover, determining how these sensitivities depend upon nanoparticle size and shape by adopting a consistent and systematic approach is also required since even subtle variations in the structure and composition of both the nanoparticle and the coating can have a dramatic effect upon the LSPR spectral characteristics. In this paper we describe experiments that, in combination with numerical modelling, allow us to further understand the factors that dictate both a particle's bulk and local sensitivity.

A large number of single nanoparticles with various sizes and shapes were fabricated by electron beam lithography (EBL) and optically characterized using dark-field spectroscopy. Scattering spectra from each individual nanoparticle were obtained for a bulk change as follows: (i) in a nitrogen environment, (ii) when immersed in methanol; and for a local change as follows: (i) in a nitrogen environment, (ii) after coating with a 2 nm layer of aluminium oxide (Al_2O_3 – also obtained in a nitrogen environment). From these data the relative shift upon immersion in solvent, and upon coating with the thin Al_2O_3 layer were found, then compared by plotting the data with respect to the position of the LSPR associated with the uncoated nanoparticle in nitrogen. This is important since for nanoparticles up to a size of 130 nm the bulk sensitivity has been found to depend only upon the initial position of the resonance and how the relative permittivity of the metal varies at this wavelength[27]. This means that in this range of particle sizes the size of the spectral shift due to a bulk change is effectively shape-independent – changing shape or aspect ratio simply tunes the LSPR spectral peak to different initial positions. Finite element modelling of the optical response of nanoparticles was also undertaken so as to provide a rigorous analysis of the experimental data by reproducing theoretically the relative shift of the LSPRs for both a bulk and local change to the environment.

Experiment

Substrate-supported Au nanoparticles were fabricated by EBL using a FEI Nova 600 dualbeam system. A polymethylmethacrylate (A2 PMMA, 950k molecular weight) resist was spin-coated onto a glass coverslip (no. 0, Agar Scientific) and then coated with a 10 nm thick layer of Au to provide a conducting layer to avoid charging of the substrate during the electron beam exposure. Following exposure, the Au conducting layer was removed using commercial Au etchant and the exposed PMMA developed in a 9:1 solution of IPA:water for 60s. Finally, 40 nm of Au was evaporated onto the substrate and, following lift-off of the PMMA resist, Au nanoparticles ranging in size from 60 nm up to 162 nm remained. Each nanoparticle was separated from its neighbours by a distance of 10 μm to enable single particle spectra to be easily obtained and to prevent inter-particle interactions.

Prior to the optical measurements being carried out the nanoparticles were chemically annealed by immersion in methanol for a period of 24 hours so as to stabilize the nanoparticle morphology. Subtle changes in shape can occur when nanoparticles are exposed to solvents that would result in anomalous LSPR shifts not solely due to a change in refractive index of the nanoparticle environment[30]. After annealing, the nanoparticles were dried in nitrogen and inserted into a flow cell consisting of two glass plates separated by ~ 50 μm. After further drying in nitrogen, dark-field spectra were obtained using a Nikon TE2000u microscope with inverted illumination and collection through a x100 dark-field dry objective. In this configuration light from a 100 W halogen bulb is incident on the particle over an angular range of 53-72 degrees. Light that was scattered by the nanoparticles was collected by the central portion of the lens and directed towards the entrance slit of a spectrometer. Attached to the exit port of the spectrometer was a CCD array that collected the dispersed light, thereby allowing spectra to be obtained from nine nanoparticles simultaneously. Further spectra were taken with the nanoparticles immersed in methanol and, after drying, a second set of spectra in nitrogen acquired to check that no

further annealing had taken place. Following this step, the nanoparticles were stored under vacuum prior to deposition of a layer of aluminium oxide. This was achieved by atomic layer deposition using a FlexAL system (Oxford Instruments) operating in thermal deposition mode. In this process reactants are pulsed through a heated chamber at 60 °C resulting in the deposition of a layer of dielectric the thickness of which is determined by the number of pulse cycles. Each cycle deposited a layer of Al_2O_3 with a thickness of 0.9 Å, so by running the process for 23 cycles a total layer thickness of 2.1 nm was deposited. The two main advantages of using Al_2O_3 as opposed to self assembled monolayers are that the refractive index can be estimated using ellipsometry and that the coating is entirely conformal with the surface of the nanoparticle. Both of these issues are less well-defined in the case of molecular binding to surfaces. Furthermore, by measuring the scattering response from individual nanoparticles that are all within an overall area of 200 μm any variability in the coating across the sample area is reduced.

Results and Discussion

Scanning electron microscope (SEM) images are shown in figure 1 of Au nanoparticles after coating with Al_2O_3; (a) a disc with a diameter of 128 nm; (b) a rod with in-plane dimensions of 119 nm x 74 nm. All of the nanoparticles fabricated for this study had a height of 40 nm as measured during evaporation of the Au using a calibrated quartz crystal thickness monitor. The nanoparticles were composed of multiple grains of single crystal Au, however the small grains shown in the images are those of a 0.5 nm coating of Au-Pd that was used to provide a conductive coating required for imaging.

The dark-field spectra of the nanoparticles shown in the SEM images are also shown in figures 1(a) and 1(b). The black and green lines correspond to bare nanoparticles in a nitrogen environment before and after immersion in methanol respectively; the red line is the spectrum for the same nanoparticle but now in a methanol environment, again with the nanoparticle bare; the blue line corresponds to a

nitrogen bulk environment, but with the nanoparticle now coated with the Al_2O_3. As expected, a red-shift occurs when the environment is altered by introducing material with a higher refractive index for both bulk and local changes. A second effect is a significant reduction in the intensity of the scattered light that is collected by the objective lens. This change is surprisingly large even for the very thin coating of Al_2O_3 deposited onto the nanoparticles and substrate, and is the opposite to what one would expect from Mie theory calculations of similarly sized coated and uncoated spheres. The scattering cross-section of Au nanoparticles calculated using Mie theory increases when the refractive index of the bulk medium is increased or a thin coating introduced[2,31]. All of the nanoparticles were characterized by obtaining SEM images and then correlating these images with the dark-field spectra. For each set of spectra the position of the LSPR peaks were found by a b-spline curve-fitting procedure. Subtracting the LSPR peak position of the uncoated nanoparticle in nitrogen from that of the uncoated nanoparticle in methanol yields the bulk shift as shown in figure 2(a). Repeating this for the coated nanoparticle in nitrogen yields the local shift as shown in figure 2(b). In both cases the relative shift is plotted as a function of the wavelength of the LSPR in nitrogen since this allows a direct comparison between individual nanoparticles – the dispersion of the gold permittivity is accounted for in this way[27]. If the relative shift was plotted as a function of nanoparticle size then a comparison between sets of differently shaped nanoparticles would be compromised; a rod with a length equivalent to the diameter of a disc would have a LSPR located at a longer wavelength and therefore the value and dispersion of the relative permittivity would be different at the LSPR position for the rod compared to the disc. From the data shown in figure 2 it is seen that in general rod-shaped nanoparticles are more sensitive than the disc-shaped nanoparticles for a bulk change and also a local change in refractive index. This is particularly clear for nanoparticles with the longest LSPR wavelengths (largest dimensions).

To confirm these results, that rods are more sensitive than discs, the optical response of the nanoparticles were simulated using a finite element modelling package[32]. To simplify the modelling and

to prevent spurious effects that arise from including a substrate using the HFSS package, transmittance spectra from infinite arrays of nanoparticles were obtained rather than scattering spectra from single nanoparticles. The periodicity of the array was small enough to ensure the data were not influenced by far-field diffraction, but large enough to minimize near-field interactions between the nanoparticles. Example transmittance spectra from the modelling are shown in figure 3(a) obtained from an array of rods with a length of 110 nm and an array of discs with a diameter of 130 nm. In both cases the pitch of the array was 300 nm. In both models the LSPR is blue-shifted relative to the experimental data shown in figure 1, this perhaps due to a suppression of the radiative damping owing to the periodic nature of the structure considered in the model. A better match between the experimental and modelled resonance positions was obtained by increasing the periodicity of the array. However, this leads to diffractive effects that alter the shape of the LSPR spectra and position of the extinction maximum[33,34,35].

As with the experimental study, numerical data were obtained for nanoparticles with a variety of sizes. For each model the relative shift was obtained for a bulk change and for a local change in the environment surrounding the substrate-supported nanoparticle. Within the model a bulk change was incorporated by adjusting the medium surrounding the nanoparticle to have a refractive index of n_{bulk} = 1.33. To simulate a local change to the environment a continuous layer was introduced so as to surround the nanoparticle and also coat the substrate. The refractive index of the layer was taken to be n_{loc} = 1.49, the same as that measured experimentally using ellipsometry for the Al_2O_3 layer. Collated data illustrating how the bulk sensitivity of the LSPR changes as the peak position of the LSPR is varied by increasing the nanoparticle size are shown in figure 3(b). At shorter wavelengths the disc and rod shapes have comparable sensitivities. However, as the LSPR in nitrogen red-shifts (as nanoparticle size increases) the sensitivity of the disc lags behind that of the rod. For a disc with a diameter of 130 nm the relative shift has saturated to a value of ~40 nm. However, the rod-shaped nanoparticles have a sensitivity that continues to increase linearly with nanoparticle size and LSPR position. As describer

earlier, this difference in the behaviour of the two shapes of nanoparticle is in contrast to what is expected for solid nanoparticles in a homogeneous environment where modelling of nanoparticles up to a size of 120 nm has shown that the bulk sensitivity is independent of the shape of the nanoparticle[27]. For the nanoparticles studied here that is certainly not the case.

In considering these results we note three key points. Firstly for a nanoparticle supported on a substrate the presence of the substrate will reduce the sensitivity when compared to an unsupported nanoparticle because a proportion of the sensing volume is now contained within the substrate. If, for nanoparticles of different shapes, the proportion of the sensing volume that is available to undergo a change is different then their sensitivity will also be different. To explore how the substrate influences the sensitivity of the nanoparticle to their environment the time-averaged scattered electric field was plotted across a plane aligned with the centre of the nanoparticle and the plane of polarization. This is shown in figures 4(a) and 4(b) for a 110 nm rod and a 130 nm disc respectively. It can be seen that the electric field extends further into the substrate for the disc than for the rod and that the proportion of the electric field associated with the LSPR within the substrate is also greater. Further modelling (data not shown) indicates that the fraction of the field in the substrate is ~40 % for the disc and ~37 % for the rod. This seems to be a subtle effect and is unlikely to fully describe the discrepancy between discs and rods.

Secondly the surface area in contact with the substrate will also affect the sensitivity – for nanoparticles with a given LSPR position a disc will have a greater surface area in contact with the substrate than a rod. For the disc typically ~32 % of the area is in contact with the substrate, in the case of the rod it is ~27 %. From this it may be inferred that the active proportion of the sensing volume for the disc would therefore be smaller[18,25]. This leads to a better agreement with the observed behaviour since as the nanoparticle size increases the difference in the proportion of contact surface area also

increases. However, there are two features of the data in figure 3(b) that indicate that this is a simplified interpretation. For smaller nanoparticles the numerical modelling indicates that discs are more sensitive than rods - this is the opposite of what would be expected by simply considering surface area. Also, that the sensitivity of the discs saturates implying that the rate of increase in the proportion of contact surface area should be increasing linearly – it does not. Further modelling is being undertaken to investigate these discrepancies more fully so as to ascertain what other effects may contribute to the suppression of the LSPR shift for discs.

Thirdly, for local sensitivity the decay length characteristics of the LSPR field profiles are important in determining the relative shift – the level of confinement of the enhanced field associated with the LSPR will partly determine the sensitivity of the LSPR. To see whether there is a greater confinement of the LSPR field at the surface for the rods compared to the discs a 110 nm rod and a 130 nm disc were modelled with a coating of Al_2O_3 with the thickness varied from 2 nm to 12 nm in 2 nm steps. These data are shown in figure 5 where the relative shift is plotted against coating thickness. As in the experiment, it is seen that the rod is more sensitive than the disc throughout. However, is there a difference in how quickly the induced shift approaches saturation, thereby giving an indication of how confined the field is to the surface of the nanoparticle? By fitting a single exponential to the data it is possible to obtain an approximate value for the characteristic decay length of the field into the external medium. The values are very similar for both the rod and the disc (7.7 ± 0.6 nm for the rod and 7.8 ± 0.8 nm for the disc) indicating that, despite having a smaller radius of curvature at the ends of the rod, the confinement of the field is similar for these particles.

Conclusion

In this paper results from experiments and finite element modelling show that, for the most part, rod-shaped Au nanoparticles supported by a substrate are more sensitive to an environmental change than

disc-shaped nanoparticles. This becomes particularly clear when the LSPR spectral position of a substrate-supported nanoparticle in nitrogen becomes > 625 nm. This difference in sensitivity is not predicted by simulations or electrostatic theory for nanoparticles embedded in a homogeneous environment[27]. We therefore attribute the disparity in sensitivity to two principal effects associated with the presence of the substrate. Firstly that the proportion of the surface area of the nanoparticle in contact with the substrate is larger for the disc than for the rod, and secondly that the proportion of the LSPR electromagnetic field in the superstrate that dictates the overall sensing volume is increased for the rod compared to the disc. Despite the rods being more sensitive than the discs to a change in the bulk environment it is shown that the field decay length into the superstrate is similar for a rod and disc with the same initial LSPR position.

Acknowledgements

The authors acknowledge the Basic Technology grant (EP/C52389X/1), 2D Attogram Surface Plasmon Resonance Imaging for funding and Oxford Instruments (Bristol) for assistance with atomic layer deposition. WLB thanks the Royal Society for their support.

References

(1) Bohren, C. F., Huffman, D. *Absorption and scattering of light by small particles*; John Wiley: New York, 1983.

(2) Kreibig, U., Vollmer, M. *Optical properties of metal clusters*; Springer-Verlag: Berlin, 1995.

(3) Murray, W. A.; Barnes, W. L. *Adv Mater* 2007, *19*, 3771.

(4) Pelton, M.; Aizpurua, J.; Bryant, G. *Laser Photonics Rev* 2008, *2*, 136.

(5) Lee, K. S.; El-Sayed, M. A. *J Phys Chem B* 2006, *110*, 19220.

(6) Jensen, T. R.; Malinsky, M. D.; Haynes, C. L.; Van Duyne, R. P. *J Phys Chem B* 2000, *104*, 10549.

(7) Mock, J. J.; Barbic, M.; Smith, D. R.; Schultz, D. A.; Schultz, S. *J Chem Phys* 2002, *116*, 6755.

(8) Murray, W. A.; Astilean, S.; Barnes, W. L. *Phys Rev B* 2004, *69*.

(9) Su, K. H.; Wei, Q. H.; Zhang, X.; Mock, J. J.; Smith, D. R.; Schultz, S. *Nano Lett* 2003, *3*, 1087.

(10) Jensen, T. R.; Duval, M. L.; Kelly, K. L.; Lazarides, A. A.; Schatz, G. C.; Van Duyne, R. P. *J Phys Chem B* 1999, *103*, 9846.

(11) Whitney, A. V.; Elam, J. W.; Zou, S. L.; Zinovev, A. V.; Stair, P. C.; Schatz, G. C.; Van Duyne, R. P. *J Phys Chem B* 2005, *109*, 20522.

(12) Murray, W. A.; Suckling, J. R.; Barnes, W. L. *Nano Lett* 2006, *6*, 1772.

(13) Mock, J. J.; Smith, D. R.; Schultz, S. *Nano Lett* 2003, *3*, 485.

(14) Raschke, G.; Kowarik, S.; Franzl, T.; Sonnichsen, C.; Klar, T. A.; Feldmann, J.; Nichtl, A.; Kurzinger, K. *Nano Lett* 2003, *3*, 935.

(15) McFarland, A. D.; Van Duyne, R. P. *Nano Lett* 2003, *3*, 1057.

(16) Liao, H. W.; Nehl, C. L.; Hafner, J. H. *Nanomedicine* 2006, *1*, 201.

(17) Willets, K. A.; Van Duyne, R. P. *Annu Rev Phys Chem* 2007, *58*, 267.

(18) Larsson, E. M.; Alegret, J.; Kall, M.; Sutherland, D. S. *Nano Lett* 2007, *7*, 1256.

(19) Nehl, C. L.; Liao, H. W.; Hafner, J. H. *Nano Lett* 2006, *6*, 683.

(20) Raschke, G.; Brogl, S.; Susha, A. S.; Rogach, A. L.; Klar, T. A.; Feldmann, J.; Fieres, B.; Petkov, N.; Bein, T.; Nichtl, A.; Kurzinger, K. *Nano Lett* 2004, *4*, 1853.

(21) Wang, H.; Brandl, D. W.; Le, F.; Nordlander, P.; Halas, N. J. *Nano Lett* 2006, *6*, 827.

(22) Sherry, L. J.; Chang, S. H.; Schatz, G. C.; Van Duyne, R. P.; Wiley, B. J.; Xia, Y. N. *Nano Lett* 2005, *5*, 2034.

(23) Sherry, L. J.; Jin, R. C.; Mirkin, C. A.; Schatz, G. C.; Van Duyne, R. P. *Nano Lett* 2006, *6*, 2060.

(24) Hao, E.; Schatz, G. C. *J Chem Phys* 2004, *120*, 357.

(25) Malinsky, M. D.; Kelly, K. L.; Schatz, G. C.; Van Duyne, R. P. *J Phys Chem B* 2001, *105*, 2343.

(26) Novo, C.; Funston, A. M.; Pastoriza-Santos, I.; Liz-Marzan, L. M.; Mulvaney, P. *J Phys Chem C* 2008, *112*, 3.

(27) Miller, M. M.; Lazarides, A. A. *J Phys Chem B* 2005, *109*, 21556.

(28) Haes, A. J.; Zou, S. L.; Schatz, G. C.; Van Duyne, R. P. *J Phys Chem B* 2004, *108*, 6961.

(29) Rindzevicius, T.; Alaverdyan, Y.; Kall, M.; Murray, W. A.; Barnes, W. L. *J Phys Chem C* 2007, *111*, 11806.

(30) Malinsky, M. D.; Kelly, K. L.; Schatz, G. C.; Van Duyne, R. P. *J Am Chem Soc* 2001, *123*, 1471.

(31) Lunt, E. A. M.; Pitter, M. C.; Somekh, M. G.; O'Shea, P. O. *J Nanosci Nanotechno* 2008, *8*, 1.

(32) Ansoft. *HFSS*.

(33) Haynes, C. L.; McFarland, A. D.; Zhao, L. L.; Van Duyne, R. P.; Schatz, G. C.; Gunnarsson, L.; Prikulis, J.; Kasemo, B.; Kall, M. *J Phys Chem B* 2003, *107*, 7337.

(34) Auguie, B.; Barnes, W. L. *Phys Rev Lett* 2008, *101*.

(35) Yizhuo, C.; Schonbrun, E.; Yang, T.; Crozier, K. B. *Applied Physics Letters* 2008, *93*.

Figure 1. Dark-field scattering spectra obtained from disc (a) and rod (b) shaped nanoparticles. Spectra correspond to uncoated nanoparticle immersed in nitrogen (black and green), methanol (red) and coated nanoparticle in nitrogen (blue). Insets show SEM images of the nanoparticles. The shoulder at wavelengths between 570 nm and 600 nm in (b) is due to the LSPR associated with the short axis.

Figure 2. Relative wavelength shift of the LSPR plotted as a function of LSPR peak position in nitrogen for (a) bulk change (nitrogen to methanol) and (b) local change (2 nm coating of aluminium oxide).

Figure 3. (a) Normal incidence transmittance spectra obtained using finite element modelling of an array of rods with a length of 110 nm (dashed) and discs with a diameter of 130 nm (solid). Spectra were obtained in nitrogen and methanol environments, as indicated. (b) Relative shift of the LSPR upon a change in the bulk environment (nitrogen to methanol) plotted against LSPR peak position in vacuum for rods (blue squares) and discs (red circles). These data should be compared with the experimentally derived data in figure 2(a).

Figure 4. Time-averaged plot of the total electric field obtained from a section through the centre of a rod (a) and a disc (b). In both cases the cross-section corresponds to the plane of polarization of the incident light. Incident field amplitude was 1 V/m.

Figure 5. Relative shift plotted against thickness of aluminium oxide coating obtained using finite element modelling for a rod with a length of 110 nm (blue squares) and a disc with a diameter of 130 nm (red circles). Solid lines are exponential fits to data points.

Figure 1.

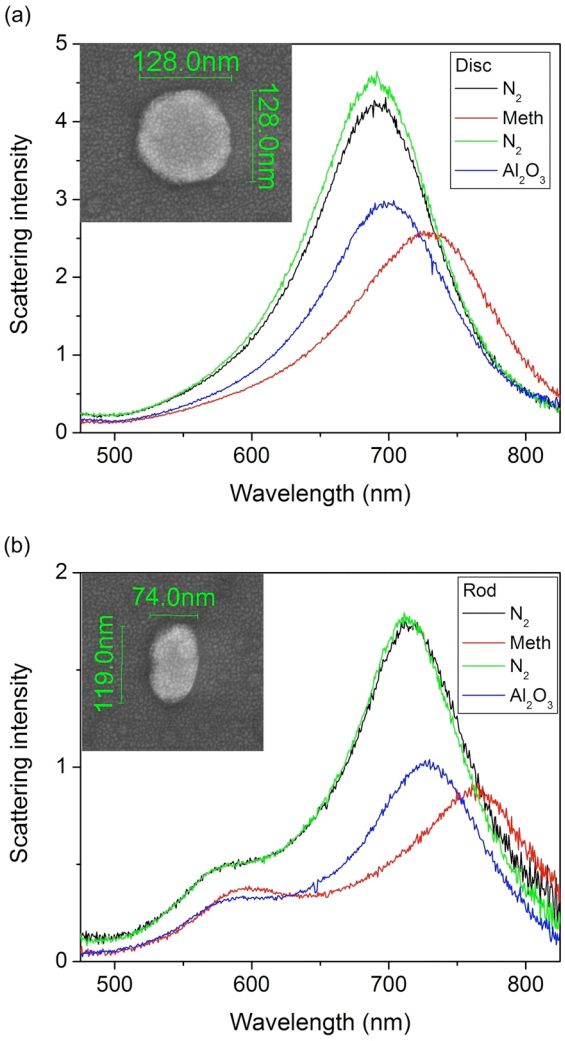
(a)
128.0nm
128.0nm
Disc
N2
Meth
N2
Al2O3
Scattering intensity
Wavelength (nm)
(b)
74.0nm
119.0nm
Rod
N2
Meth
N2
Al2O3
Scattering intensity
Wavelength (nm)

Figure 2

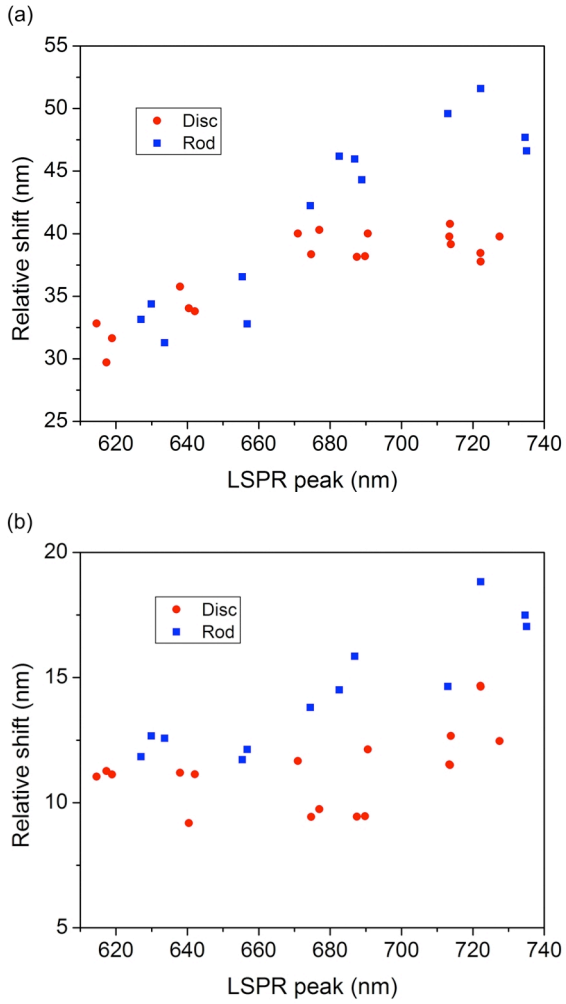
(a)
Disc
Rod
Relative shift (nm)
LSPR peak (nm)
(b)
Disc
Rod
Relative shift (nm)
LSPR peak (nm)

Figure 3

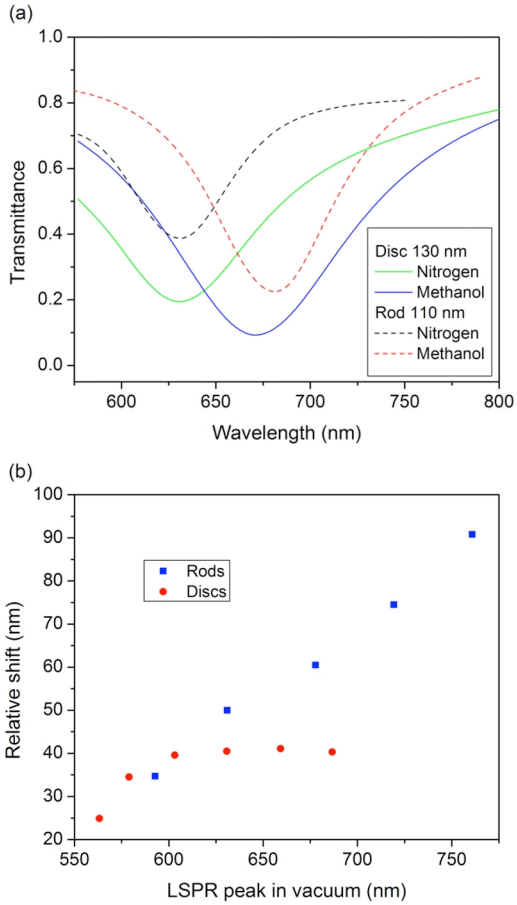
(a)
Transmittance
Wavelength (nm)
Disc 130 nm
Nitrogen
Methanol
Rod 110 nm
Nitrogen
Methanol
(b)
Relative shift (nm)
LSPR peak in vacuum (nm)
Rods
Discs

Figure 4

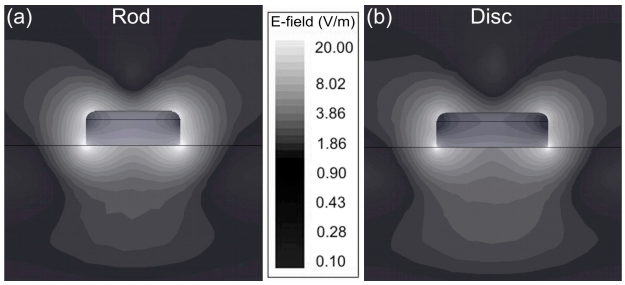

Figure 5

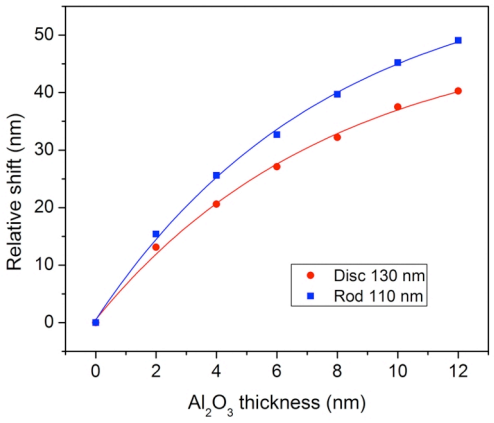
Relative shift (nm)
50
40
30
20
10
0
0
2
4
6
8
10
12
Al2O3 thickness (nm)
Disc 130 nm
Rod 110 nm